Near Surface Geophysics

Near Surface Geophysics, 2020, **18**, 249–259 doi: 10.1002/nsg.12094

High resolution 3D subsurface mapping using a towed transient electromagnetic system - tTEM: case studies

Pradip Kumar Maurya*, Anders Vest Christiansen, Jesper Pedersen and Esben Auken

HydroGeophysics Group, Institute of Geoscience, Aarhus University, C.F. Møllers Allé 4, Building 1120, DK-8000 Aarhus C, Denmark

Received May 2019, revision accepted January 2020

ABSTRACT

Geophysical methods are routinely applied for investigation of near surface in areas of infrastructure, water supply, artificial infiltration, farming, waste deposits, construction, etc. A new towed transient electromagnetic tool, called ‘tTEM’, provides rapid, efficient, high-resolution imaging of subsurface hydrogeology, and can deliver densely spaced profiles of resistivity. These profiles can be used to map a three-dimensional subsurface in high resolution. In this paper, we present three case studies where the towed transient electromagnetic system was used to map the subsurface at the hectare scale. In the first case, we used towed transient electromagnetic to map raw materials in the northern Jutland, Denmark. The survey was carried out to map possible sand and gravel deposits. In the towed transient electromagnetic models, the potential sand/gravel targets are identified as high resistive bodies in the top 30 m. These bodies can have significant lateral variation at scales much less than one hundred metres. In the second case study, towed transient electromagnetic was used to map the thickness of a protecting clay layer above an aquifer in Vildbjerg, a town in the central part of Denmark. Results show that the overlying clay layer has sufficient thickness (>15 m) to protect the underlying aquifer from pesticide pollution in the area. Finally, in the third case study, we used towed transient electromagnetic for mapping geology in the vicinity of a landfill. The inversion results reveal a hitherto unknown buried valley-like feature within the top 30 m of the subsurface that was not identified by older, regional TEM surveys – a feature that can have significant impact on the water flow.

Key words: 3D, TEM, Electromagnetics.

1 INTRODUCTION

Detailed investigations of Earth’s shallow subsurface are in high demand, as most human activities are concentrated in this zone. For example, the development of infrastructure, artificial infiltration, agricultural activities, waste disposal and surface water–groundwater interaction (Brantley, Goldhaber and Ragnarsdottir 2007) generally occur within a few tens of metres beneath the earth surface. These activities may have adverse impacts on the environment and local ecosystems. For example, high nutrient loads from farming practices may deteriorate groundwater quality if the underlying aquifer is vulnerable (Burkart and Kolpin 1993; Worrall and Kolpin 2004; Leone *et al.* 2009). Similarly, waste disposal sites such as landfills can contaminate ground and surface water (Milosevic *et al.* 2012; Bjerg *et al.* 2014; Maurya *et al.* 2017).

In many countries, drinking water is sourced from groundwater aquifers. Maintaining a high water quality and sufficient quantity is often a challenging task for water managers, who require detailed knowledge of the subsurface in

*E-mail: pradip.maurya@geo.au.dk

order to set sustainable groundwater management guidelines. This is especially relevant when dealing with the issues related to high nutrients loads due to farming (Gaines and Gaines 1994; Spieles and Mitsch 1999; Jackson, Preston and Thompson 2004; Xie and Ringler 2017). To maintain clean water, one needs to do a detailed vulnerability mapping of the aquifers, to identify areas with high risk of aquifer pollution and areas controlling the movement of nutrients in the subsurface. Similarly, accessing the risk associated with contaminated sites and optimizing the location of investigation and remediation boreholes require detailed geological knowledge of the extent and spreading rates of the leachate or contaminants (Stempvoort, Ewert and Wassenaar 1993). For instance, if the distribution of clay and sand deposits is known in the vicinity of the contaminant source, one can predict the pathways for the movement of the water and the leachate.

Infrastructure development, such as buildings, highways or rail roads, requires basic raw (construction) materials (sand and gravel primarily). Local authorities must constantly replenish their diminishing supplies of construction materials. For sustainable exploration of raw materials, there is a growing need for subsurface mapping. In the past, several case studies have investigated the subsurface prior to excavation of the construction materials (Ellefsen, Lucius and Fitterman 1998; Beresnev, Hruby and Davis 2002; Chambers *et al.* 2012). In these case studies, geophysical methods (such as electrical methods) were used for pre-investigation of the area for the presence of possible raw material deposits.

Over the past few decades, near surface geophysical methods and downhole surveys have played a vital role in subsurface mapping. The target depth for these investigations ranges from surface to a few hundred metres. For human activities, the top 50–60 m is most important and detailed investigation of this zone is becoming increasingly important. In the top 50–60 m, the most commonly used geophysical techniques are various electrical and electromagnetic methods. Electrical resistivity tomography (ERT) is a technically robust method and is capable of covering this depth range with relatively high resolution (Loke *et al.* 2013; Glover 2015). However, due to time-consuming data collection, most often only a few two-dimensional profiles are collected. Actual area coverage of more than a few hectares would be very time demanding (Auken *et al.* 2014; Maurya *et al.* 2017) - as a result, three-dimensional ERT data collection is generally limited to a few hectares.

Application of transient electromagnetic (TEM) techniques for near surface investigations has been growing in environmental investigations and mineral explorations (Fitterman and Labson 2005; Auken *et al.* 2006; Christensen and Halkjær 2014). Over the past few decades, a significant advancement in the core technology of TEM instruments, airborne as well as ground-based, has been achieved. Airborne electromagnetic methods have been quite popular and frequently used (Auken, Boesen and Christiansen 2017), but due to the relatively large footprints they are mainly used for regional surveys and are not suited for sub-hectare resolution. Also, the very shallow layers (<10 m) are not well resolved.

There are few geophysical instruments providing high spatial resolution with continuous data recording, ultimately supplying areal coverage with high resolution. Two such direct-current resistivity systems are the PACES system (Sørensen 1996; Christensen and Sørensen 2001) and the OhmMapper by Geometrics Inc. (Garman and Purcell 2004). These instruments can cover larger areas but with limited depth of investigation (DOI), ~25 m for PACES and ~8 m for OhmMapper. Resistivity systems like these can obtain higher DOI, but at the expense of longer layouts pulled by the vehicle in front. For example, the PACES system has an ~100 m tail to drag in order to achieve a 15–20 m DOI. Frequency-domain electromagnetic systems such as DUALEM-421 can be towed by an all-terrain vehicle (Saey *et al.* 2015; Christiansen *et al.* 2016) and can effectively map larger areas but again with very limited DOI (3–7 m).

Recently, Auken *et al.* (2019) presented a new towed TEM (tTEM) system with a DOI of about 70 m, depending on the resistivity structures. The tTEM system can map the subsurface with great resolution both vertically (shallow resolution about 2–3 m) and horizontally (down to 10×10 m). The tTEM system has been used for various purposes in Denmark, USA and Sweden. To demonstrate the utility of this system, we will present three tTEM case studies:

1 A case study mapping raw (construction) materials in Stendal Mark situated in Northern Demark.

2 A study to assess aquifer vulnerability by mapping of overlying clay layers on farm fields in Vildbjerg, Central Denmark.

3 A general geological mapping in the vicinity of a landfill in Trige, close to Aarhus, Denmark.

2 METHOD AND MATERIALS

2.1 Study sites

The locations of the three study sites are shown in Figure 1. The first site is located in northern Jutland in the area of Stendal Mark. The aim of this survey was to map the spatial extent of gravel deposits and clay/till cover layers. The

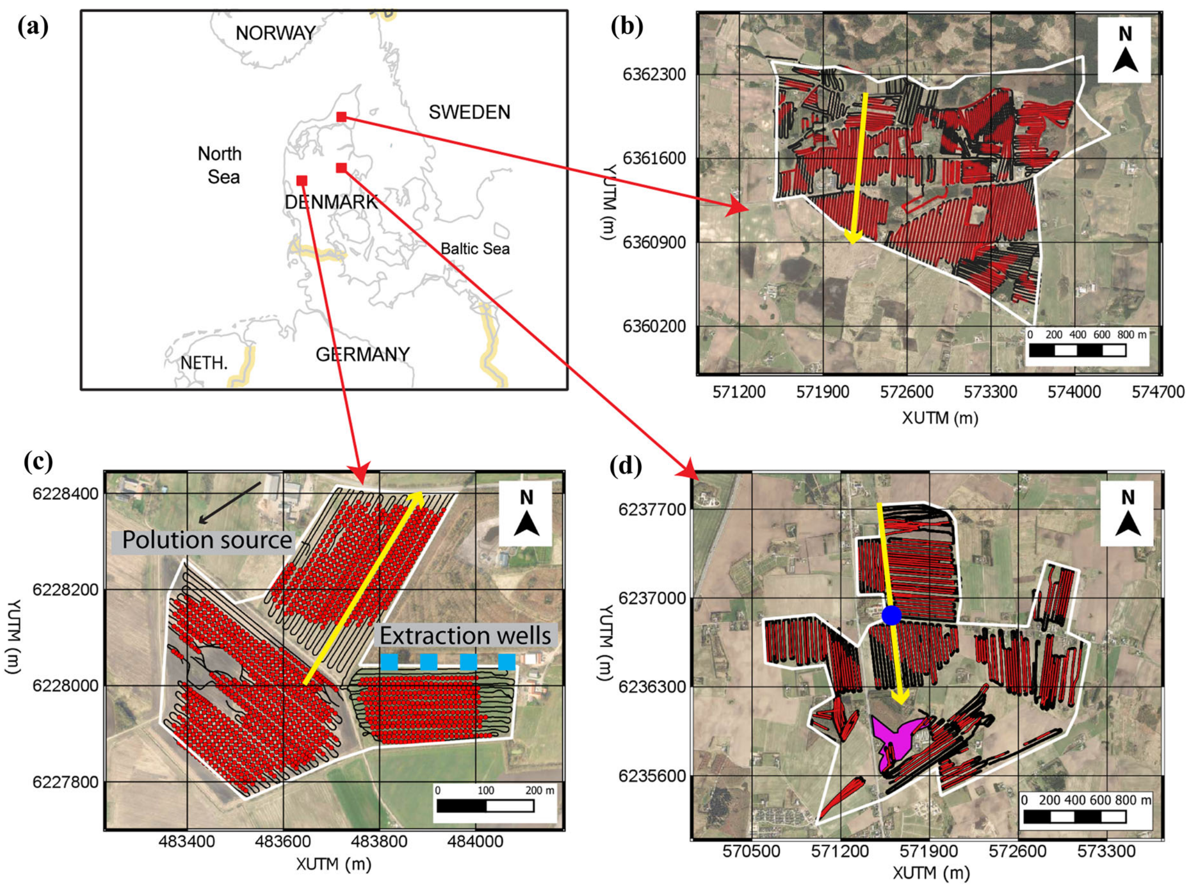

Figure 1 (a) Location of the study sites on the map, (b) Stendal Mark, (c) Vildbjerg, and (d) Trige with a landfill location outlined in pink. For subplots (b)–(d), tTEM lines (raw data) are in black, tTEM models (after processing) in red, the white line outlines the survey areas and the yellow arrows in (b) and (d) indicate resulting sections shown in the examples, and (c) shows the example of data section shown in Figure 3.

mapping was conducted as a part of Region Northern Jutland raw material plan, which was designed to ensure that there were sufficient areas where one can extract raw material for the upcoming 12 years of consumption. This drives the need for a detailed sand and gravel mapping over large areas. The survey is composed of several farmers' fields spanning a total area of 364 hectares, see Figure 1(b) and Table 1. The geology of the area is dominated by glacial sediments. The

Table 1 Field statistics of the tTEM surveys

Study Area	Area (ha)	Line Length (km)	Acquisition Time (hour)	Average Line Spacing (m)
Stendal Mark	364	~82	18.1	25
Vildbjerg	25	~24.1	2.1	10
Trige	210	~65	12.5	25

layer sequence from the surface is typically composed of a glacio-fluvial sand/gravel layer with varying thickness, which is followed by till layers. Often the sequence is repeated and in some areas there is a clay or till cover on top of the sand and gravel. In such a setting, the exact thickness of the clay cover is of great importance to estimate if the sand and gravel deposits are profitable to extract.

The second site is located in Vildbjerg, a small town in the central part of Jutland. The survey was carried out near a reported pesticide pollution, see Figure 1(c). The water flow direction is oriented southeast from the polluted site – directly towards the town's waterworks extraction site that provides drinking water for 4000 inhabitants. The geology of the area consists of a top mica clay layer underlain by quartz sand deposits from which groundwater is extracted. As per borehole information in the area, the thickness of the top mica clay layer may vary in the range from 8 to 20 m. Groundwater is extracted from a quartz sand layer situated at 45–60 m depth, which constitutes the primary aquifer. The aim of the survey was to obtain a three-dimensional image of the thickness and continuity of the clay layer in order to investigate the aquifer's vulnerability to potential pesticide pollution. If the clay cover is more than 15 m thick, the aquifer is considered safe.

The third area is located in Trige, close to Aarhus. The survey area is located around a landfill, which is situated in the southern part of the area, see Figure 1(d). The geological setting in this area is basically glacial layers on top of a pre-quaternary sequence of clays and marls (Høyer *et al.* 2015). The quaternary sequence is often related to incised valleys that are both shallow and deep (up to 130 m) (Jørgensen and Sandersen 2006). The Quaternary deposits are clay tills and fine-to-coarse grained meltwater deposits. Incised valleys filled with meltwater sands and gravels are the main aquifers for the drinking water supply in the area. The aim of the survey was to identify potential pathways for pollution leachate from the landfill; hence a detailed sand and clay distribution mapping was undertaken.

2.2 The tTEM system

tTEM is a towed transient electromagnetic system developed by the HydroGeophysics Group at Aarhus University (Auken *et al.* 2019). Figure 2 shows the layout of the system. The system has a one-turn 2×4 m^2 transmitter loop and a 670 kHz receiver coil (suspended induction coil) in a 9 m offset configuration. The Rx coil is a 56 by 56 cm^2 multi-turn coil with an area of 5 m^2. The Tx and Rx coils are mounted on sleds for a smooth ride during operation. For data positioning, two GPSs are mounted on the Tx and the Rx coil. The system is towed by an all-terrain vehicle (ATV), at a speed of 15–20 km/h. All electronic instruments (transmitter and receiver) and battery power supply are placed on the back of the ATV. An Intel NUC PC with 4 cores runs the data acquisition and the navigation system. The PC is connected to a tablet PC through a remote desktop which is controlled and monitored by the driver. The system uploads the data directly to the cloud by a 4G network.

The system transmits a low and a high moment (LM, HM) current pulse to achieve both shallow and deep information. The LM transmits 2.8 A with a turn-off time of 2.6 μs and a first usable gate at 4 μs (times from beginning of the ramp-down, so the gate opens at 1.05 μs from end of ramp and is 0.65 μs wide) while the HM transmits 30 A. The repetition frequencies for the LM and HM pulse are 2160 and 660 Hz. The transmitter is water cooled to keep the current ramp repeatable and the transmitter temperature at 45°C (±2°C) and the current at 30 A (±1 A).

2.3 Data acquisition, processing and inversion

Figure 1 shows the position of the towed transient electromagnetic (tTEM) lines for all three areas. On the fields, the all-terrain vehicle (ATV) was driven mostly on tractor tracks, so the line spacing was between 20 and 25 m except at the Vildbjerg area where the line spacing was 10 m. The data were collected with an average speed of 10–15 km /h. In Table 1, details about the surveys are given.

While operating over the rough fields, mechanical vibrations and rotations introduce noise in the tTEM signal. However, it has been shown by Auken *et al.* (2019) that with the high repetition frequency and a low-pass filter, this noise is suppressed effectively. Furthermore, the low-pass filter also includes a notch filter to suppress the 50 or 60 Hz power line harmonic noise. After the noise suppression, raw transients are stacked and a standard deviation (STD) is obtained for each gate value based on the size of stack. These data STDs are used in the inversion process as data weights.

Processing of tTEM data follows the scheme presented by Auken *et al.* (2009) for airborne transient electromegnetic data. The data were processed using the Aarhus Workbench software (www.aarhusgeosoftware.dk). Figure 3 shows an example of tTEM data with both low moment and high moment. During processing, couplings to man-made infrastructure (Christiansen, Auken and Sørensen 2006b) are removed in the raw stacked data (grey data points in figure 3). Data close to the end-of-line turns are removed as well because the ATV gets too close to the TX frame causing data coupling. Finally, the data are averaged over approximately 2.5 seconds to further suppress random noise and reduce the number of soundings, resulting in approximately 10 m spaced TEM soundings. After this, a preliminary laterally constrained inversion is done to confirm the quality of the processing and, if necessary, further culling of the data is performed.

The tTEM data are inverted using the one-dimensional spatially constrained inversion algorithm by Viezzoli, Auken and Munday (2009), implemented in an integrated inversion and modelling code AarhusInv (Auken *et al.* 2015). The forward response of the TEM data incorporates modelling of the key parameters of the system transfer functions such as transmitter waveform, transmitter/receiver timing, low-pass filters, gate widths and system geometry. All tTEM data were inverted using a smooth multi-layer model consisting of

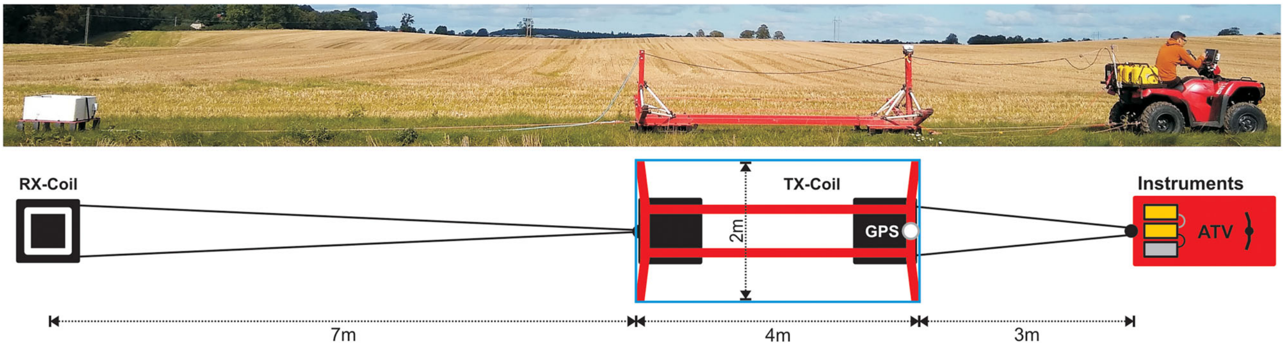

Figure 2 The tTEM system. Top: a side view of the system ready to operate in the field. Bottom: sketch of the top view of the system (modified from Auken *et al*. 2019).

25 layers with logarithmically increasing thicknesses starting at 1 m and with the last layer boundary at 150 m. The depth of investigation was estimated for each model, following Christiansen and Auken (2012).

3 RESULTS

3.1 Raw material mapping: Stendal mark

Figures 4 and 5 show the results of the towed transient electromagnetic survey from the Stendal Mark area. The survey was carried out to find the volume of possible gravel deposits in the area. Deposits correspond to high-resistivity bodies. In Figure 4, a resistivity model section along a 1000 m profile is shown. Data from profile coordinates 300–450 m and 800–850 m are missing due to a coupling caused by a buried cable. It can be seen that the thickness of the high resistivity layer (>200 Ωm) varies strongly on a scale around only 1000 m. It also appears to be an area with glacial disturbance, as evidenced by the presence of tilted and thrusted layers. All this information is of course vital in the location and design of a gravel extraction area. The grain size in the bodies has not yet been confirmed by investigation drillings and there is a chance that they consist of silty sediments and not sand and gravel. Results from such drilling is expected in 2020, hence they cannot be shown here.

Figure 5 shows the overall distribution of possible gravel deposits as high-resistivity iso-surfaces in three dimensions. The iso-surface volume is created by extracting the high-resistivity values (>200 Ωm) from a full three-dimensional volume created by kriging interpolation of the resistivity models onto a regular grid. The model positions are shown on the top of the surface by dotted lines. The resulting image shows overall that the gravel deposits are thicker in north-eastern and south-western part of the area.

3.2 Aquifer vulnerability assessment, Vildbjerg

Figure 6 shows spatially constrained inversion results from the Vildbjerg survey area. The three-dimensional (3D) resistivity volume is created using the same procedure as described in Section 3.1. A satellite image is draped onto the 3D volume and the model positions are indicated with dots. The arrow shows the groundwater flow direction going from the point source contamination towards the drinking water extraction wells. The 3D volume is cut along the flow direction and perpendicular to the flow direction in order to better visualize the structure. The view angle is from the pollution source towards the water extraction wells. From this view, it is clear that the towed transient electromagnetic (tTEM) inversion model shows variable thickness of the protecting mica clay layer (<25 Ωm) and that this layer completely confines the underlying aquifer.

Figure 7 shows a map with the calculated thickness of the mica clay layer based on the tTEM models (25 Ωm threshold). In addition to the existing borehole B1, two new boreholes B2 and B3 were made after the tTEM survey. The thickness of the capping clay layer observed in the boreholes B1, B2 and B3 are 23.8, 21.3 and 22.5 m, respectively, which is in very good agreement with clay thickness map shown in Figure 7.

Vildbjerg Waterworks extracts water from the quartz sand deposits between 45 and 60 m depth. As seen in the clay thickness map (Fig. 7), the thickness of the mica clay cap between the pollution source and the water wells is more than 15 m, and there are no 'windows' in the clay layer. Consequently, there is minimal risk for dispersal of the pesticide pollution towards the extraction drillings. This knowledge would have been difficult and costly to gain solely by means of drillings and would have risked creating connected pathways from the upper contaminated region to the lower drinking water aquifer.

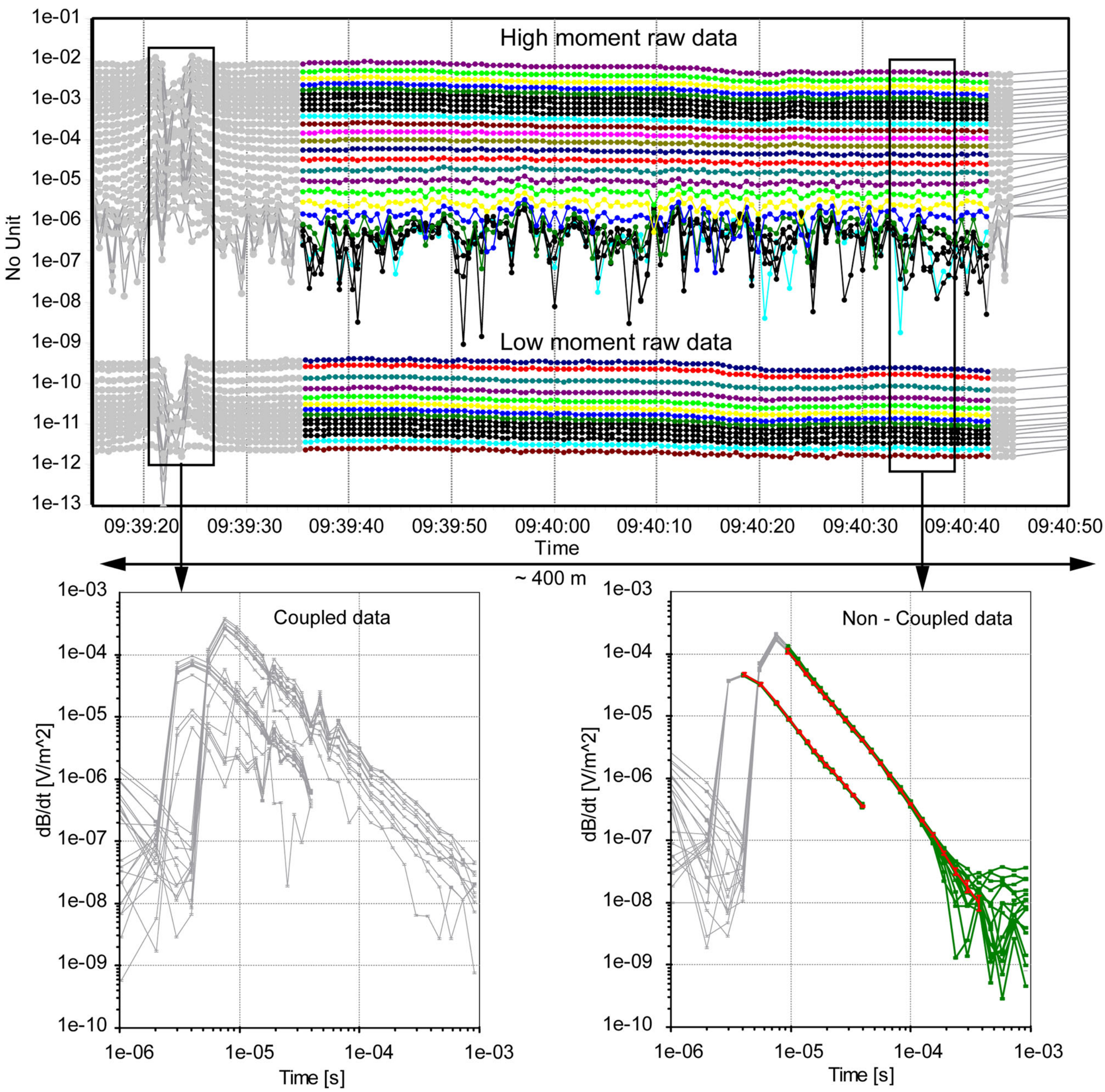

Figure 3 Example of tTEM data section from Vildbjerg. Top: the data in gray are removed. A typical example of coupled and non-coupled data shown in the bottom. In non-coupled data, green decays are the raw data soundings, whereas the red decay is the average sounding.

3.3 General geological mapping, Trige

The third towed transient electromagnetic (tTEM) survey area around the Trige landfill has been a subject of regional geological mapping before. Multiple historical TEM datasets were collected over time for general geological mapping of the area (Høyer *et al.* 2015). These datasets include ground-based transient electromagnetic (TEM) soundings and SkyTEM data. Databases with historical models were fetched from the Danish national geophysical database (GERDA) (ww.geus.dk). Figure 8(a) shows a mean resistivity map at an elevation of 35–40 m from the historical data. The boundary of the tTEM survey area is shown by the dashed black line. In Figure 8(b), a mean resistivity map derived from tTEM spatially constrained inversion (SCI) models are superimposed on top of the historical background resistivity map at the same elevation interval.

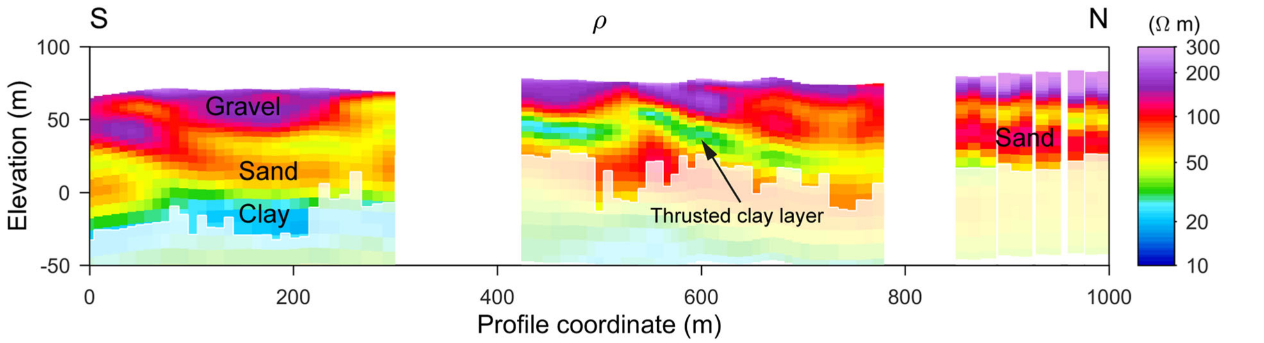

Figure 4 Resistivity model section in Stendal Mark. The location of the profile is shown in Figure 1(b), model below the DOI is faded with the white colour.

The inversion models from the historical studies reveals that the area contains deeply incised buried valleys in a depth range of 70–300 m. These buried valleys are seen as high-resistive bodies in low-resistive environments (Høyer *et al.* 2015). The structures are below the depth of investigation of the tTEM system, and we do not expect to see them; however, Figure 8(a,b) shows significant differences within the tTEM survey area. A high resistivity, 100 m wide, valley-like feature sitting on the plateau of the clay surface is seen in Figure 8(b), but missing in Figure 8(a). The valley was missed by the large-footprint, low-density older campaigns with ground-based TEM (mainly pulled array TEM called PaTEM) and SkyTEM. The tTEM system sees it because of the smaller footprint and denser sampling.

A resistivity section across this feature is shown in Figure 9. Also borehole lithology is shown. This section is created from an interpolated three-dimensional (3D) resistivity volume based on the tTEM SCI models (Fig. 9b) and the models from the historical dataset (Fig. 9a), respectively. As seen, the lithology and the resistivity models in Figure 9(a) agrees quite well with the lithological boundaries of top sand layer, sand till layer and top of the clay layer. Note that the shallow buried valley-like feature seen in Figure 9(b) is missing both in the borehole and in the resistivity section of Figure 9(a) because it is located just next to this valley. Hence, without

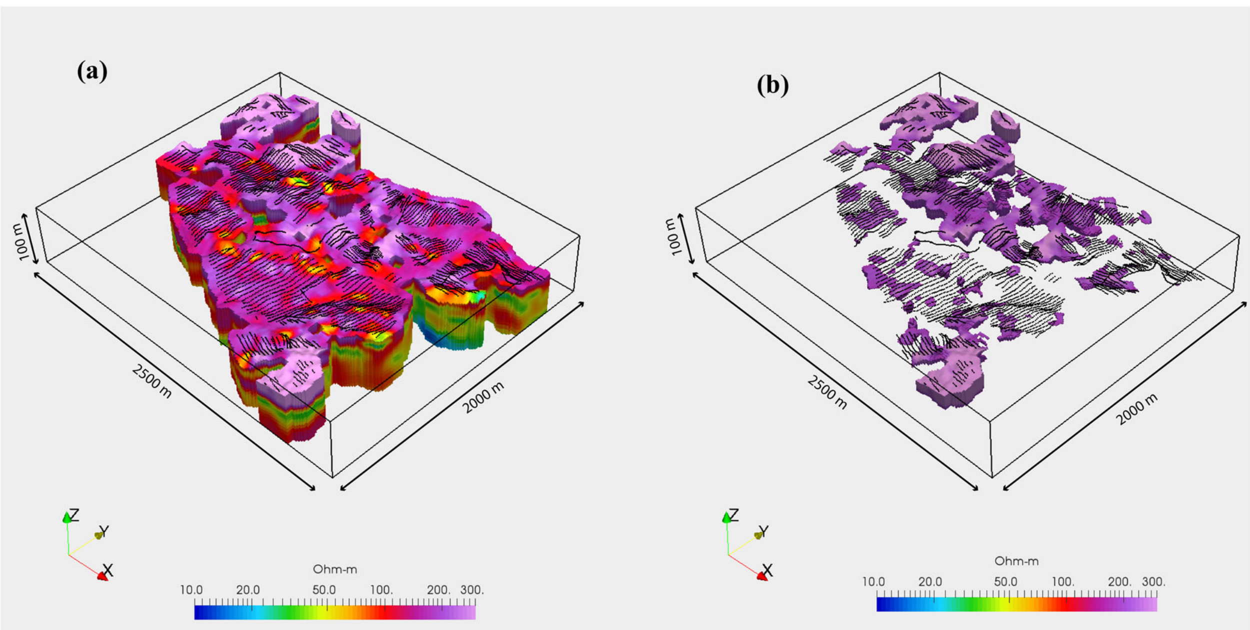

Figure 5 (a) 3D volume of resistivity model of Stendal Mark area and (b) iso-volume of high resistivity materials (>200 Ωm) extracted from 3D volume. The black dots are the positions of the tTEM models.

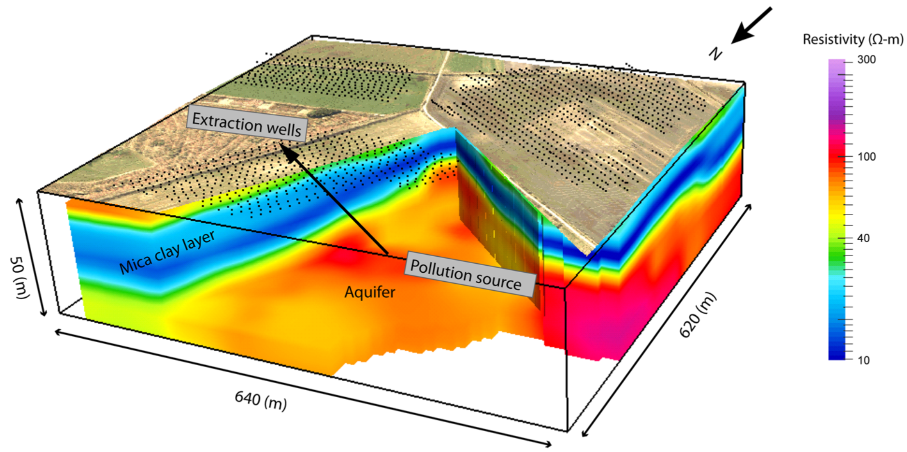

Figure 6 3D view of the resistivity volume created using kriging interpolation of the 1D resistivity model from the Vildbjerg survey. The mica clay layers have a resistivity <25 Ωm. The arrow shows the groundwater flow direction.

the tTEM survey, the valley would not have been discovered, although it has the potential to be an important path for outflow of contamination from the landfill.

4 DISCUSSION AND OUTLOOK

In the above case histories, we presented the application of the towed transient electromagnetic (tTEM) method for a number of different purposes. The system is very easy to deploy and can cover larger areas with very good horizontal and vertical resolution. In a moderate resistivity environment, the system has a depth of investigation (DOI) of 60–70 m. In areas with very conductive layers, the DOI of tTEM is less, possibly 30–40 m. Electromagnetic (EM) coupling noise and disturbance from power lines and fences in the tTEM signal (Danielsen *et al.* 2003; Christiansen, Auken and Sørensen 2006a) are one

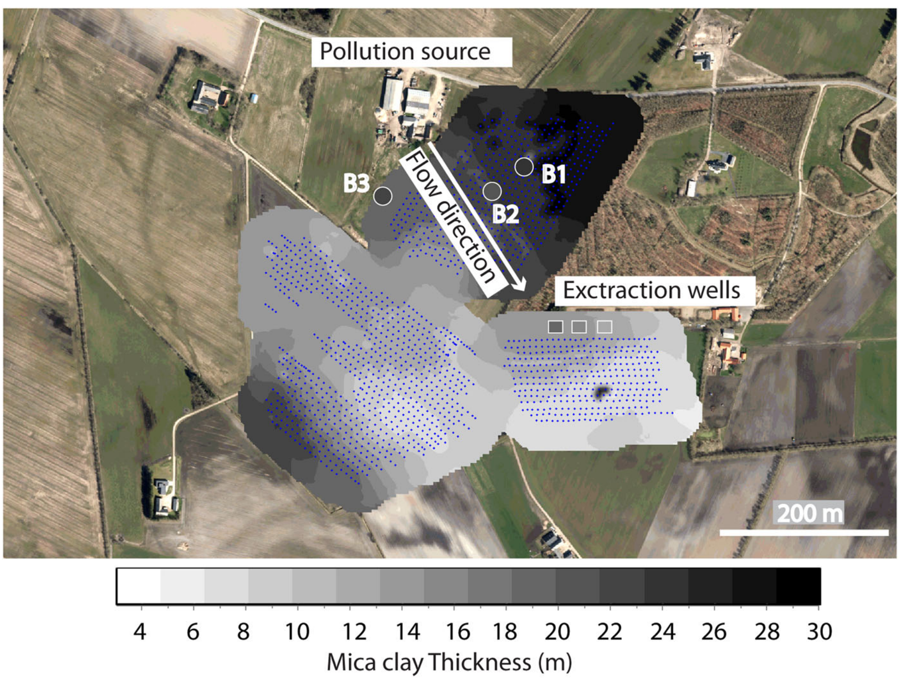

Figure 7 Thickness of the mica clay layer in Vildbjerg survey area, derived from tTEM inversion models. Circles outlined with white colour (B1–B3) are the lithological boreholes and the squares are the drinking water extraction wells. The inner colour fill in the circles and in the squares are according to the colour scale of clay thickness. The blue dots are position of the tTEM models.

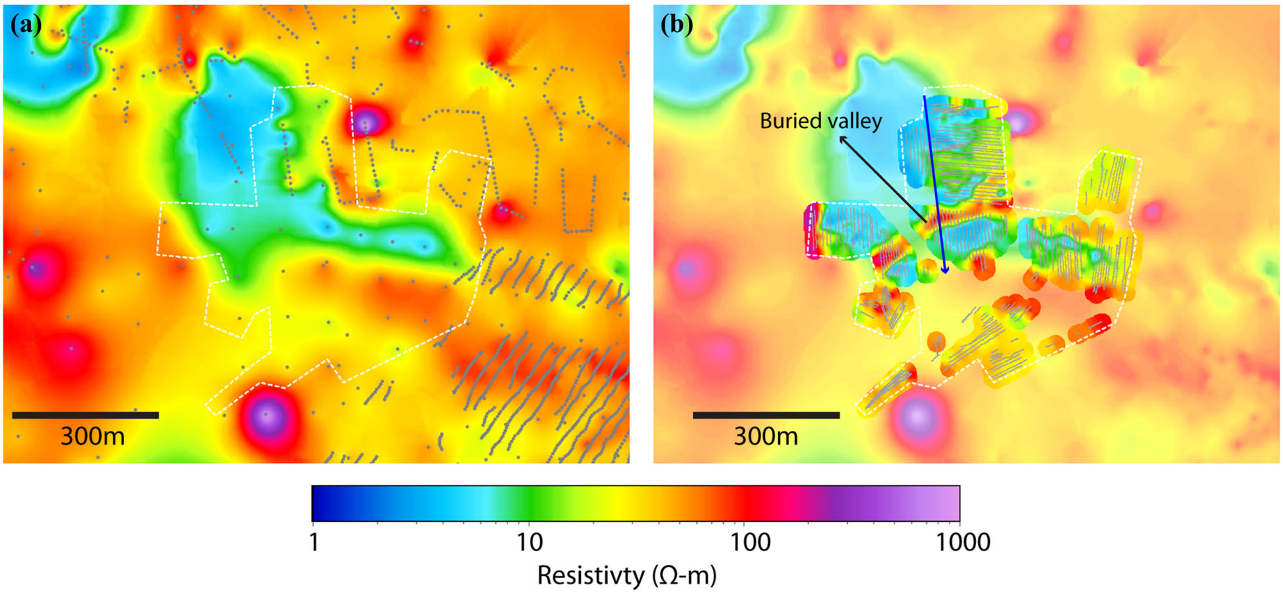

Figure 8 (a) Mean resistivity map at elevation interval 35–40 m from historical TEM models. (b) Mean resistivity map at elevation interval 35–40 m, created from tTEM models. The dashed line indicates the survey boundary of the tTEM data and blue arrow marks the profile shown in the Figure 9. The grey dots in both figures shows the model positions.

of the fundamental problems just like for other EM methods. They must be removed during data processing, which means that transient electromagnetic soundings close to power lines, housing and other any infra-structure must be carefully processed. Based on experience, the distance at which the power lines can be neglected is around 50 m, whereas it is in the range of 100–150 m for airborne and large-loop ground based systems. This reduced sensitivity is explained by the small transmitter coil of the tTEM system from where the primary field decays faster compared to systems with a larger loop, thus

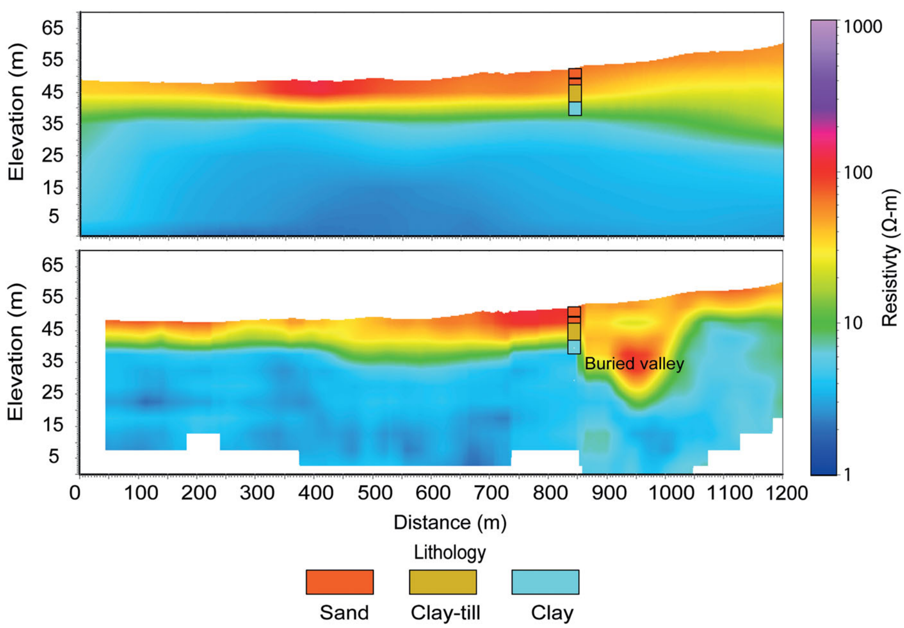

Figure 9 (a) Resistivity section from the historical models and (b) resitivty section from tTEM SCI inverted models. Both sections show one litholog in good accordence with the resistivity sections.

inducing less power in the power lines and fences. The other main limitation of the tTEM method is accessibility. Like any ground-based method, tTEM is restricted to map where land access is granted and possible. In forested areas, only the forest roads would typically be accessible and in the open land some areas might be too wet to be accessed by an all-terrain vehicle. Aside from this, the last limitation is being granted access to map the fields. In Denmark, most fields would be inaccessible from the beginning of April till August/September depending on the crops on the fields. Obviously, this timing will vary from place to place and also vary with crop type.

The raw material mapping in Stendal Mark presented a suitable target for tTEM as the gavel/sand deposit are underlain by clay layers which are well resolved by the TEM method in general and the thickness of the raw material can be estimated. This might not be case for other field sites if a sufficient conductivity contrast is not present. The high lateral resolution of the tTEM system showed a detailed clay thickness mapping in Vildbjerg for assessing the vulnerability of the aquifers to a point-source pollution. This level of detail is unlikely to be achieved by other ground-based TEM or airborne methods, since they lack the horizontal resolution needed. This is also evident in the case of the tTEM survey in Trige, where previous studies conducted at the regional scale completely missed the presence of a shallow buried valley-like structure. When building a detailed high-resolution groundwater model, this buried valley-like structure would be considered an important structure. In fact, the main purpose of the survey conducted in Trige was to build the groundwater model around the landfill area (see Figure 1) to assess the risk of spreading of contaminants. Therefore, finding these possible shallow buried valleys is crucial.

5 CONCLUSION

In this paper, we presented three successful applications of the towed transient electromagnetic (tTEM) tool for different purposes: mapping of raw materials, aquifer vulnerability assessment, and mapping of geology in general. The tTEM system is fast and efficient in mapping at hectare scale with high resolution. The tTEM data are processed following well-established processing scheme for airborne electromagnetic data and inverted using the spatially constrained inversion algorithm.

The case study of Stendal Mark area shows that tTEM can be an efficient tool for mapping raw materials within 60–70 m depth. The inversion model has shown that high resistivity areas, which likely correspond to sand and gravel deposits in this area, are in the top 30 m. The thickness of these sand deposits varies strongly even within a few hundred metres, thus highlighting the need for high horizontal resolution. In the second case study, tTEM was used to map the thickness of a protecting clay layer. We prove that the top-capping clay layer has sufficient thickness (>15 m) to protect the underlying aquifer from pesticide pollution in the area. Finally, we use tTEM to map geology in the vicinity of a landfill. The inversion results reveal a hitherto unknown, shallow buried valley-like feature within 30 m from the surface that was not identified in older, regional TEM surveys.

ACKNOWLEDGEMENTS

The study has been funded by the Innovation Fund Denmark projects rOpen (Open landscape nitrate retention mapping), MapField (Field-scale mapping for targeted N-regulation and management) and the Interreg VB North Sea Region project TOPSOIL. We are also grateful to Jens Demant Bernth from Orbicon A/S, Rikke Ellemann-Biltoft from Region Northern Jutland and Central Denmark Region for the permission to show the mapping examples. Finally, the Aarhus University center for water technologies, WATEC, has supported the developments.

ORCID

Pradip Kumar Maurya
https://orcid.org/0000-0002-7887-6219

REFERENCES

Auken E., Boesen T. and Christiansen A.V. 2017. A review of airborne electromagnetic methods with focus on geotechnical and hydrological applications from 2007 to 2017. *Advances in Geophysics* **58**, 47–93.

Auken E., Christiansen A.V., Fiandaca G., Schamper C., Behroozmand A.A., Binley A. *et al.* 2015. An overview of a highly versatile forward and stable inverse algorithm for airborne, ground-based and borehole electromagnetic and electric data. *Exploration Geophysics* **2015**, 223–235.

Auken E., Christiansen A.V., Westergaard J.A., Kirkegaard C., Foged N. and Viezzoli A. 2009. An integrated processing scheme for high-resolution airborne electromagnetic surveys, the SkyTEM system. *Exploration Geophysics* **40**, 184–192.

Auken E., Doetsch J., Fiandaca G., Christiansen A.V., Gazoty A., Cahill A.G. *et al.* 2014. Imaging subsurface migration of dissolved CO2 in a shallow aquifer using 3-D time-lapse electrical resistivity tomography. *Journal of Applied Geophysics* **101**, 31–41.

Auken E., Foged N., Larsen J.J., Lassen K., Maurya P., Dath S. *et al.* 2019. tTEM — A towed transient electromagnetic system for detailed 3D imaging of the top 70 m of the subsurface *Geophysics* **84**, 1942–2156.

Auken E., Pellerin L., Christensen N.B. and Sørensen K.I. 2006. A survey of current trends in near-surface electrical and electromagnetic methods. *Geophysics* **71**, G249–G260.

Beresnev I.A., Hruby C.E. and Davis C. 2002. The use of multi-electrode resistivity imaging in gravel prospecting. *Journal of Applied Geophysics* **49**, 245–254.

Bjerg P.L., Albrechtsen H.J., Kjeldsen P., Christensen T.H. and Cozzarelli I.M. 2014. 11.16 - The biogeochemistry of contaminant groundwater plumes arising from waste disposal facilities. *Treatise on Geochemistry* (eds H.D. Holland and K.K. Turekian), pp. 573–605. Elsevier.

Brantley S.L., Goldhaber M.B. and Ragnarsdottir K.V. 2007. Crossing disciplines and scales to understand the critical zone. *Elements* **3**, 307–314.

Burkart M.R. and Kolpin D.W. 1993. Hydrologic and land-use factors associated with herbicides and nitrate in near-surface aquifers. *Journal of Environmental Quality* **22**, 646–656.

Chambers J., Wilkinson P., Weller A., Meldrum P., Kuras O., Ogilvy R. *et al*. 2012. Characterising sand and gravel deposits using electrical resistivity tomography (ERT): case histories from England and Wales. Extractive Industry Geology Conference, 166–172.

Christensen N.B. and Halkjær M. 2014. Mapping pollution and coastal hydrogeology with helicopterborne transient electromagnetic measurements. *Exploration Geophysics* **45**, 243–254.

Christensen N.B. and Sørensen K.I. 2001. Pulled array continuous electrical sounding with an additional inductive source: an experimental design study. *Geophysical Prospecting* **49**, 241–254.

Christiansen A., Pedersen J.B., Auken E., Søe N.E., Holst M.K. and Kristiansen S.M. 2016. Improved geoarchaeological mapping with electromagnetic induction instruments from dedicated processing and inversion. *Remote Sensing* **8**, 1022.

Christiansen A.V. and Auken E. 2012. A global measure for depth of investigation. *Geophysics* **77**, WB171–WB177.

Christiansen A.V., Auken E. and Sørensen K. 2006a. The transient electromagnetic method. *Groundwater Geophysics* (ed. R. Kirsch), pp. 179–225. Springer.

Christiansen A.V., Auken E. and Sørensen K. 2006b. From resistivity to clay thickness - An inversion approach. *19th Annual Symposium on the Application of Geophysics to Engineering and Environmental Problems (SAGEEP)*. EEGS.

Danielsen J.E., Auken E., Jørgensen F., Søndergaard V.H. and Sørensen K.I. 2003. The application of the transient electromagnetic method in hydrogeophysical surveys. *Journal of Applied Geophysics* **53**, 181–198.

Ellefsen K.J., Lucius J.E. and Fitterman D.V. 1998. *An Evaluation of Several Geophysical Methods for Characterizing Sand and Gravel Deposits*. U.S. Geological Survey.

Fitterman D.V. and Labson V.F. 2005. Electromagnetic induction methods for environmental problems. In: *Near-Surface Geophysics Part I* (ed. D.K. Butler), pp. 301–356. SEG.

Gaines T.P. and Gaines S. 1994. Soil texture effect on nitrate leaching in soil percolates. *Communications in Soil Science and Plant Analysis* **25**, 2561–2570.

Garman K.M. and Purcell S.F. 2004. Applications for capacitively coupled resistivity surveys in Florida. *The Leading Edge* **23**, 697–698.

Glover P.W.J. 2015. 11.04 Geophysical properties of the near surface earth: electrical properties. In: *Treatise on Geophysics* (ed. G. Schubert), pp. 89–137. Elsevier.

Høyer A.-S., Jørgensen F., Sandersen P.B.E., Viezzoli A. and Møller I. 2015. 3D Geological modelling of a complex buried-valley network delineated from borehole and AEM Data. *Journal of Applied Geophysics* **2015**, 94–102.

Jackson C., Preston N. and Thompson P.J. 2004. Intake and discharge nutrient loads at three intensive shrimp farms. *Aquaculture Research* **35**, 1053–1061.

Jørgensen F. and Sandersen P.B.E. 2006. Buried and open tunnel valleys in Denmark-erosion beneath multiple ice sheets. *Quaternary Science Reviews* **25**, 1339–1363.

Leone A., Ripa M.N., Uricchio V., Deák J. and Vargay Z. 2009. Vulnerability and risk evaluation of agricultural nitrogen pollution for Hungary's main aquifer using DRASTIC and GLEAMS models. *Journal of Environmental Management* **90**, 2969–2978.

Loke M.H., Chambers J.E., Rucker D.F., Kuras O. and Wilkinson P.B. 2013. Recent developments in the direct-current geoelectrical imaging method. *Journal of Applied Geophysics* **95**, 135–156.

Maurya P.K., Rønde V.K., Fiandaca G., Balbarini N., Auken E., Bjerg P.L. *et al*. 2017. Detailed landfill leachate plume mapping using 2D and 3D electrical resistivity tomography - with correlation to ionic strength measured in screens. *Journal of Applied Geophysics* **138**, 1–8.

Milosevic N., Thomsen N.I., Juhler R.K., Albrechtsen H.J. and Bjerg P.L. 2012. Identification of discharge zones and quantification of contaminant mass discharges into a local stream from a landfill in a heterogeneous geologic setting. *Journal of Hydrology* **446**, 13–23.

Saey T., Van Meirvenne M., De Smedt P., Stichelbaut B., Delefortrie S., Baldwin E. *et al*. 2015. Combining EMI and GPR for non-invasive soil sensing at the Stonehenge World Heritage Site: the reconstruction of a WW1 practice trench. *European Journal of Soil Science* **66**, 166–178.

Sørensen K.I. 1996. Pulled array continuous electrical profiling. *First Break* **14**, 85–90.

Spieles D.J. and Mitsch W.J. 1999. The effects of season and hydrologic and chemical loading on nitrate retention in constructed wetlands: a comparison of low-and high-nutrient riverine systems. *Ecological Engineering* **14**, 77–91.

Stempvoort D.V., Ewert L. and Wassenaar L. 1993. Aquifer vulnerability index: a GIS-compatible method for groundwater vulnerability mapping. *Canadian Water Resources Journal* **18**, 25–37.

Viezzoli A., Auken E. and Munday T. 2009. Spatially constrained inversion for quasi 3D modelling of airborne electromagnetic data - an application for environmental assessment in the Lower Murray Region of South Australia. *Exploration Geophysics* **40**, 173–183.

Worrall F. and Kolpin D.W. 2004. Aquifer vulnerability to pesticide pollution—combining soil, land-use and aquifer properties with molecular descriptors. *Journal of Hydrology* **293**, 191–204.

Xie H. and Ringler C. 2017. Agricultural nutrient loadings to the freshwater environment: the role of climate change and socioeconomic change. *Environmental Research Letters* **12**, 104008.